



University of Kentucky
UKnowledge

Civil Engineering Faculty Publications

Civil Engineering

2-1-2017

US Residential Building Air Exchange Rates: New Perspectives to Improve Decision Making at Vapor Intrusion Sites

Rivka Reichman
University of Kentucky

Elham Shirazi
University of Kentucky, elham.shirazi@uky.edu

Donald G. Colliver
University of Kentucky, dcolliver@uky.edu

Kelly G. Pennell
University of Kentucky, kellypennell@uky.edu

Right click to open a feedback form in a new tab to let us know how this document benefits you.

Follow this and additional works at: https://uknowledge.uky.edu/ce_facpub

 Part of the [Civil and Environmental Engineering Commons](#), and the [Environmental Sciences Commons](#)

Repository Citation

Reichman, Rivka; Shirazi, Elham; Colliver, Donald G.; and Pennell, Kelly G., "US Residential Building Air Exchange Rates: New Perspectives to Improve Decision Making at Vapor Intrusion Sites" (2017). *Civil Engineering Faculty Publications*. 15.
https://uknowledge.uky.edu/ce_facpub/15

This Review is brought to you for free and open access by the Civil Engineering at UKnowledge. It has been accepted for inclusion in Civil Engineering Faculty Publications by an authorized administrator of UKnowledge. For more information, please contact UKnowledge@lsv.uky.edu.

US Residential Building Air Exchange Rates: New Perspectives to Improve Decision Making at Vapor Intrusion Sites

Notes/Citation Information

Published in *Environmental Science: Processes & Impacts*, v. 19, issue 2, p. 87-100.

This journal is © The Royal Society of Chemistry 2017

The copyright holder has granted the permission for posting the article here.

The document available for download is the authors' post-peer-review final draft of the article.

Digital Object Identifier (DOI)

<https://doi.org/10.1039/C6EM00504G>



HHS Public Access

Author manuscript

Environ Sci Process Impacts. Author manuscript; available in PMC 2018 February 22.

Published in final edited form as:

Environ Sci Process Impacts. 2017 February 22; 19(2): 87–100. doi:10.1039/c6em00504g.

US Residential Building Air Exchange Rates: New Perspectives to Improve Decision Making at Vapor Intrusion Sites

Rivka Reichman^a, Elham Shirazi^a, Donald G. Colliver^b, and Kelly G. Pennell^{*,a}

^aUniversity of Kentucky, Department of Civil Engineering, Lexington, KY 40506

^bUniversity of Kentucky, Department of Biosystems and Agricultural Engineering, Lexington, KY 40503

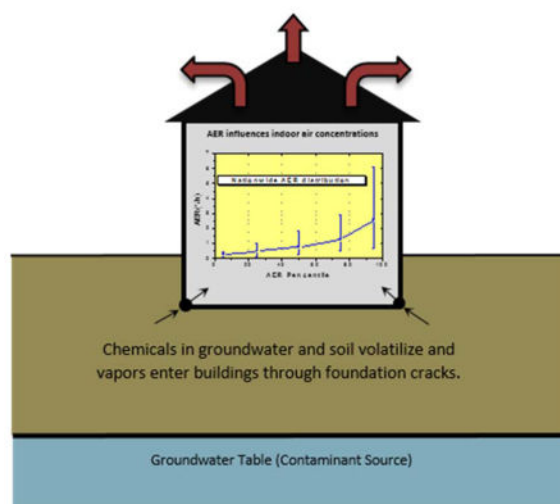
Abstract

Vapor intrusion (VI) is well-known to be difficult to characterize because indoor air (IA) concentrations exhibit considerable temporal and spatial variability in homes throughout impacted communities. To overcome this and other limitations, most VI science has focused on subsurface processes; however there is a need to understand the role of aboveground processes, especially building operation, in the context of VI exposure risks. This tutorial review focuses on building air exchange rates (AERs) and provides a review of literature related building AERs to inform decision making at VI sites. Commonly referenced AER values used by VI regulators and practitioners do not account for the variability in AER values that have been published in indoor air quality studies. The information presented herein highlights that seasonal differences, short-term weather conditions, home age and air conditioning status, which are well known to influence AERs, are also likely to influence IA concentrations at VI sites. Results of a 3D VI model in combination with relevant AER values reveal that IA concentrations can vary more than one order of magnitude due to air conditioning status and one order of magnitude due to house age. Collectively, the data presented strongly support the need to consider AERs when making decisions at VI sites.

Graphical Abstract

Variations in building air exchange rates influence indoor air concentrations and vapor intrusion exposure risks.

*Corresponding Author: kellypennell@uky.edu, (859) 218-2540.



INTRODUCTION

Vapor intrusion (VI) involves indoor air (IA) contamination resulting from the migration of volatile organic compounds (VOCs) from contaminated groundwater and soil into overlying buildings, and can pose health risks to building occupants. Measuring IA concentrations to evaluate VI exposure risks is complicated by many factors, including temporal variations in VOC concentrations, multiple chemical sources (some of which are not related to VI), as well as changes in building operation, among others. One of the most challenging aspects of collecting IA data is related to spatial and temporal variability of VOC concentrations¹⁻³, and there is a lack of definitive guidance for indoor air sampling strategies that effectively address this variability².

Amidst the variability in IA concentration, VI site investigations often focus on the collection and analysis of subsurface samples along with IA data, and, in some cases VI modeling, as part of a multiple lines of evidence approach to evaluate the potential for VI exposure risks^{e.g.4}. Recently, the importance of building operation has gained recognition within the VI community⁵⁻¹⁵. Newer approaches for characterizing VI exposure risks have begun focusing on building operation (e.g. 11-13); however, the United States (US) federal and state regulatory documents (e.g. 1) lack well-defined guidance about how to incorporate building operation into site-specific investigations.

The goal of this tutorial review paper is to connect the field of VI characterization with the established field of indoor air quality research related to building air exchange rates (AERs). AERs are widely acknowledged throughout the indoor air literature as an important parameter controlling indoor air quality¹⁶⁻²⁶. Here, we provide information for the VI community about the importance of considering the role of building AERs when evaluating VI exposure risks.

BACKGROUND

VI Conceptual Model

VOC migration from contaminated groundwater and soil into overlying buildings includes three main processes: 1) vapor transport through soil from a chemical source; 2) VOC vapor entry into building; and, 3) dilution/dispersion within the building. Vapor transport through the soil is predominantly governed by vapor diffusion and is determined by the properties of contaminant and the soil. Vapor entry into the building occurs by combination of diffusion and convective transport mechanisms. The convective transport is driven by the pressure difference between the inside of the building and the outside of the building. This pressure difference, known as the driving force for vapor entry, is caused by a combination of the stack effect (which occurs due to air density gradient due to the temperature difference between the outside and inside of the building), wind effects, and building ventilation processes. Once soil vapors enter the building, it undergoes a mixing that is influenced by the AER. A detailed description of VI conceptual model is provided in 2015 USEPA VI guidance¹.

Current VI Site-specific Exposure Risk Assessment Approach

USEPA¹ recommends using multiple lines of evidence to make decisions at VI sites. This approach includes the collection of many types of data and may include modeling, with a strong interest in characterizing IA exposure risks. Field data have shown substantial spatial (house-to-house) and temporal variability in IA concentrations. For instance, Johnston and Gibson³ found a one-order-of-magnitude variability in tetrachloroethylene (PCE) concentrations in IA across both space and time among the residential study homes in San Antonio, Texas. Holton *et al*² conducted extensive IA sampling for 2.5 years in a single house overlying a dilute chlorinated solvent plume (10–50 µg/L TCE). IA concentrations varied by 3 orders of magnitude (>0.01–10 ppbv TCE). One source of IA variability has been linked to preferential pathways, in particular the unintentional entry of sewer gas entering indoor spaces *e.g.* 12,27. However, experimental results have also shown that induced building-pressure variations influence the temporal and spatial variability of both radon and VOC concentrations in sub-slab and IA⁷. Factors that may be responsible for variations in building pressures include, among others, changes in atmospheric conditions (*e.g.*, temperature, wind and barometric pressure) and changes in building conditions (*e.g.*, fluctuation in building AER due to resident behavior/heating, ventilation and air-conditioning (HAVC) system operation)^{8–15}. Numerical results using 3D model and actual field barometric pressure and wind data as input have shown two to four orders of magnitude variability across the instantaneous IA concentrations and about an order of magnitude variability for 24 h averages for a month-long simulation and non-degrading chemical¹⁴.

The conceptual understanding of VI is predominately focused on subsurface transport and this perspective has been incorporated into many VI models^{5, 28–32}, with few exceptions *e.g.* 10, 14. Virtually all VI models use Equation 1 to calculate IA concentration, which relies on two parameters that describe the building characteristics; building AER and the indoor space volume⁵. Many simulations will use a default value such as of 0.5^{28–35} or 0.25³³ for

AER; however, as will be discussed later, these default values do not adequately account for the uncertainty and variability in AER.

$$C_{\text{indoor}} = \frac{A_{\text{ck}} J_{\text{T}}}{\text{AER} \cdot V_{\text{b}} + Q_{\text{ck}}} \quad (1)$$

Where,

J_{T} – Soil gas flux from the subsurface into the building (M/L²/t)

AER – Air exchange rate (1/t)

A_{ck} – Area of the crack in the floor that permits soil gas entry (L²)

Q_{ck} – Soil gas flow through crack into building (L³/t)

V_{b} – Volume of the enclosed building space (L³)

AER is a controlling factor for energy consumption and IA quality for all buildings, not only at VI sites. Air quality studies have shown variation in AER based on geographical differences in weather conditions, building characteristics, and occupant behavior^{16–26}. AER depends on many factors including meteorological conditions (e.g. indoor/outdoor temperature differences and wind speed) building characteristics (e.g. tightness of the building envelope, type of mechanical ventilation, surrounding terrain, and local wind sheltering) and occupant behavior (e.g. opening windows and the mechanical ventilation operating manner). As will be discussed later these factors are related to the physical driving forces of the airflows.

Typical AER values reported in VI literature (presented in Table 1) show that most studies are restricted to the range of values recommended by USEPA¹ as part of the screening process to identify “at-risk” buildings for VI exposures. The range that USEPA recommends is at the lower end of typical AER distributions found in the air quality literature (presented in Table 3 and Figure 2). This lower range is reasonable for conservative risk assessment screening purposes but does not adequately reflect the AER values published literature (e.g., Isaacs *et al.*¹⁹).

USEPA’s conservative AER range (0.18–1.26 1/h) is not intended to be used as an assumption when interpreting IA concentration data or evaluating a range of possible exposure scenarios. However, this range has been commonly used during VI studies (Table 1). The *assumption* that a building has a low AER value (i.e. 0.18–1.26 1/h) when a building has a low *measured* IA VOC concentration may incorrectly suggest that a building has a low potential for VI exposure risks. As shown in Equation 1, a high AER may result in a low indoor air concentration. But, in this scenario, the potential for VI exposure risks could actually be quite high.

It is important to note that when AERs are altered, then the indoor air concentration could change. While the general trends can be expected to be inverse (e.g. as AER increases, IA decrease and vice versa), exact relationships cannot be easily extracted because as discussed

below, AERs are influenced by many factors; and, some of those factors also impact J_T (Equation 1). But, by understanding that AERs can span much broader ranges (Table 3 and Figure 2) than conservative risk screening values, the VI community can become better informed when making decisions at VI sites.

Further, the challenge of house-to-house variability has long been reported as a risk communication challenge during VI investigations. When engaging with VI communities and communicating exposure risks to homeowners and building occupants, regulators and practitioners could share broader perspectives about the well-established variability of AERs, and the role that AERs play in the variability of IA quality.

Building Air Exchange Rates (AER)

AER is the rate at which the whole house volume air exchanges with the outdoor air. When the time unit is hours, AER is referred to as air changes per hour (ACH, 1/h). Air exchange is the combination of two processes: infiltration and ventilation. As shown in Equation 1, the VI community often shows Q_{ck} (first term in denominator) as separate from total air flow rate through the building envelope (second term in denominator); however Q_{ck} is included in that as part of the formal definition of infiltration.

Infiltration refers to uncontrolled outdoor air flow through unintentional openings in the building envelope, that is, leaks. These leaks include the cracks and penetrations that exist in all buildings, including those that are of importance for VI (e.g. Q_{ck}). In residential buildings, many common leak locations have been established as major sources of infiltration, including: the main envelope area; wall, roof and floor junctions; doors and windows; penetrations through the envelope, including electrical components, as well as chimneys, wood burning stoves, etc^{17, 36}. An extensive study by Bailly *et al.*³⁶ conducted at over 35,000 French single family houses reported that leaks through windows and doors were responsible for the majority of total measured building leaks, followed closely by leaks through electrical components. Over the period of one year, this same study showed little fluctuation in infiltration rates (reported as airtightness) based on monthly measurements, suggesting that building tightness is not (typically) biased by measurement season.

Ventilation includes natural ventilation and mechanical ventilation; and can be highly variable depending on a range of factors. For purposes herein, natural ventilation is outdoor airflow through intentional openings such as open windows, and is driven by weather condition. Mechanical ventilation is airflow induced by powered equipment. These definitions are fairly commonly accepted; however alternate definitions do exist. A detailed description of infiltration and ventilation is provided in the *ASHRAE Handbook - Fundamentals*¹⁷.

In residential construction, energy-saving trends have resulted in homes being tighter and less prone to infiltration. As a result, ventilation systems are an important part of providing adequate AERs. ASHRAE standard 62.2³⁷ establishes ventilation airflow and measurement requirements for residential buildings. The required whole house ventilation rate is based on the number of bedrooms in the house, and the number of occupants. There are a variety of ways to meet the airflow requirements set forth by this standard, either through mechanical

systems or via natural forces. The exact nature of a residential ventilation system will play important role in the overall AER; however, because of the complexity of residential ventilation systems, a thorough discussion is beyond the scope of this work. The reader is directed to Russell (2005)³⁸ which provides a review of residential ventilation systems.

In 2012, Stratton *et al.*³⁹ conducted a study in California to evaluate whole house ventilation rates, as well as air flow from various components (exhaust fans, hoods, etc.) and documented the accuracy of measurement techniques that comply with ASHRAE 62.2³⁷. Thirteen (13) of the fifteen (15) homes met the ASHRAE 62.2 requirements. As an example, to be compliant with ASHRAE 62.2, a 2000 ft² home with 3 bedrooms would require a whole building airflow of 50 ft³/min. In the 15 houses (3–4 bedroom homes) that were measured, the whole-building ventilation rates ranged from 32 to 116 ft³/min, which demonstrates the variability in ventilation rates among housing stocks.

Another important aspect in ventilation variability is occupant behavior. Bathroom fans, kitchen hoods and other airflow devices can have relatively high flow rates (10s of ft³/min), as compared to whole-house ventilation rates. While these components may only be operated intermittently, their operation should be considered, especially if IA concentrations are being measured while they may be operating.

In terms of natural ventilation, opening windows and doors also can have an important impact on AERs. Reed *et al.*⁴⁰ reported that opening windows were substantially more important than stack or wind effects in changing AERs in building. They also reported that the effect of opening windows was important for homes located in both the east and west geographical areas of the US; and quantified the effect based on the dimensions of the opened area. The effect of opening windows was more recently investigated by Jeong *et al.*⁴¹ and highlighted the role of building occupants seeking to control their own environments. Opening windows is an effective way to control temperature when mechanical ventilation systems are ineffective, inefficient or too expensive. Within VI communities, building occupants also desire to control their indoor environments and VI practitioners should anticipate IA concentrations may be influenced by changes in AER due to building occupant behaviors.

Driving Forces for AER

AER is driven by pressure differences across the building envelope caused by: 1) air density differences due to temperature differences between indoor and outdoor air (stack effect); 2) wind; and, 3) the operation of mechanical equipment. A brief description of these forces is given in the following subsections, further information can be found in *ASHRAE Handbook - Fundamentals*¹⁷.

Stack effect—Temperature difference between indoor and outdoor causes density differences, and results in a pressure difference. During the heating season (winter), indoor air is warmer and therefore lighter than outdoor air, thereby creating a pressure difference across the building envelope. As a simple representation, the building acts like a chimney, exhausting warm air in the upper part of the building, and drawing in cool outdoor air in the lower part of the building (Figure 1A). During the cooling season (summer), the flow

directions are reversed and generally lower, because the indoor-outdoor temperature differences are smaller. The height at which the interior and exterior pressures are equal is called the neutral pressure level (NPL). Above this point (during the heating season) the interior pressure is greater than the exterior, below this point, the greater exterior pressure causes airflow into the building (Figure 1A). The location of the NPL at zero wind speed is a structure dependent parameter. If the openings are uniformly distributed vertically, they have the same resistance to airflow, and there is no internal airflow resistance, the NPL is at the mid-height of the building (Figure 1A).

Pressure difference (P_s , (M/L.t²)) caused by stack effect at height H is computed using equation 2 based on *ASHRAE Handbook - Fundamentals*¹⁷.

$$P_s = \rho g (H_{NPL} - H) \left(\frac{T_{in} - T_{out}}{T_{in}} \right) \quad (2)$$

Where ρ (M/L³) is outdoor air density, g (L/t²) is gravitational acceleration, H_{NPL} (L) is the location in the building envelope where there is no indoor-to-outdoor pressure difference, and T_{in} (absolute temperature) and T_{out} (absolute temperature) are the indoor and outdoor temperatures, respectively.

Wind effect—As wind flows around a building, it generally produces a positive pressure (over-pressure) on the windward side of a building and negative pressure (under-pressure) on the leeward side. The pressure on the other sides can be either negative or positive, depending on wind angle, local terrain, and building shape. These pressure differences (as compared to the inside of the building) cause inflow (infiltration) on the windward side(s) and outflow (exfiltration) on the leeward side(s) (Figure 1B).

Pressure difference (P_w , (M/L.t²)) caused by wind effect at height H is calculated using equation 3 based on *ASHRAE Handbook - Fundamentals*¹⁷:

$$P_w = \frac{1}{2} \rho U_H^2 (C_{p,out} - C_{p,in}) \quad (3)$$

Where $C_{p,out}$ (dimensionless) is the wind pressure coefficient at a leakage point on the building, $C_{p,in}$ (dimensionless) is the interior wind pressure coefficient, C_p values are a function of location of the paths on a building surface and wind direction. A detailed description about C_p values is provided in *ASHRAE Handbook - Fundamentals*¹⁷.

U_H (L/t) is the wind velocity at the reference height H (L) that can be calculated as follows:

$$U_H = U_{met} \left(\frac{\delta_{met}}{H_{met}} \right)^{\alpha_{met}} \left(\frac{H}{\delta} \right)^{\alpha} \quad (4)$$

In which, U_{met} (L/t) is the wind velocity at the height of H_{met} (L), H_{met} is the reference height at the meteorological station (Usually 10m above ground level); δ_{met} (L) and α_{met} (dimensionless) are the atmospheric boundary layer thickness and the exponent at meteorological station, respectively. δ (L) and α (dimensionless) are the corresponding values for the local building terrain which can be found in table 1, chapter 24 of *ASHRAE Handbook - Fundamentals*¹⁷.

Mechanical systems—Mechanical systems can be “unbalanced” (e.g., exhaust fans that force air out, or supply fans that force it into the building) or “balanced” (e.g., systems that have both exhaust and supply fans). Excess exhaust airflow depressurizes the building by creating a net negative pressure and excess supply airflow pressurizes the building by creating a net positive pressure. If a perfect balanced ventilation system is installed (which is rare on-site), the internal pressure of the building does not change, but an unbalanced system changes the internal pressure and consequently affects infiltration rate through the leaks.

Combining driving forces—The flow rate through an opening in the building envelope is a subject to the total pressure differences at the location, which is the sum of all the driving forces. Figure 1C qualitatively shows the addition of stack (Fig. 1A) and wind (Fig. 1B) driving forces for a simplified case where the NPL is in the mid-height, there is no mechanical ventilation, the wind pressure coefficients are uniform on each side, and the magnitude of pressure differences caused by stack effect and wind are equal (which is rare in reality). Total airflow is similar to that with the wind acting alone, but significantly larger than the airflow due only to the stack effect. The total pressure difference through each opening due to stack and wind effects can be estimated by adding P_s and P_w as follows:

$$\Delta P = P_s + P_w \quad (5)$$

The infiltration rate (Q_f (L³/t)) created by wind- and stack-induced pressure differential can be estimated using a power law relationship⁴²:

$$Q_f = \kappa \Delta P^n \quad (6)$$

Where,

κ – Leakage coefficient ((L³/t).(M/L.t²)⁻ⁿ)

n – Power law flow exponent.

Accurate calculation of flow rates through a real building envelop based on the driving forces described above requires a considerable computational capability and excessive amount of input that makes it non-realistic for large scale usage. To overcome this difficulty simplified models were developed (e.g., see AER Estimation Models).

The relative importance of the wind and stack pressures in a building depends on building characteristics (e.g., height, shape, internal resistance to vertical airflow and location of openings), local terrain and the immediate shielding of the building. For any building, there

will be ranges of wind speed and temperature difference for which the building's infiltration is dominated by the stack effect, the wind or a regime in which the driving pressures of both must be considered.

The effect of mechanical ventilation on the total envelope pressure difference depends on the direction of the ventilation flow and differences in these ventilation flows among the zones of the building. Pressurizing or depressurizing all levels uniformly has little effect on the pressure differences across floors and vertical shaft enclosures, but pressurizing individual stories increases the pressure drop across these internal separations. In a balanced system, the total flow rate (Q_t) is the addition of flow created by balanced mechanical system and the infiltration.

$$Q_t = Q_f + Q_{bm} \quad (7)$$

In which, Q_f is the flowrate through the leaks in a building caused by wind and stack effects and Q_{bm} is the flow rate created by balanced mechanical systems.

An unbalanced system influences the indoor air pressure in a building which consequently interacts with flows induced by wind and stack effect (infiltration). There are several numerical approaches that attempt to combine infiltration and unbalanced mechanical ventilation rates (Table 1 in Hurel *et al.*⁴³). These models exhibit a wide range of errors, which demonstrates the difficulty in capturing the complexity of various factors, including: building envelop leakage, weather conditions, leakage distributions and strengths of mechanical ventilation. Hurel *et al.*⁴³ used a subadditivity function to calculate the total airflow caused by infiltration and unbalanced mechanical ventilation in single family detached buildings which reduced the long-term errors to 1% or less.

Summary of Residential AERs

AER Distributions—AER distributions are usually expressed using the lognormal distribution. Several key existing datasets for US residential AER distribution are summarized in Table 2. These datasets are a collection of various projects at different regions in the US that were collected on the course of two types of programs: human exposure programs and residential energy efficiency (e.g. BNL, DEAR, and RIOPA) and weatherization assistance programs (WAPs) (e.g. LBNL). In human exposure programs, AER is measured using the perfluorocarbon tracer method (PFT). WAPs are assessing the building leakage or airtightness and the metric used is the normalized leakage (NL). AER and NL can be related using the scaling factor (SF) model²⁰ (e.g., Empirical models, see AER Models). None of the AER datasets statistically represent the characteristics of houses in the US as a whole¹⁶; however these data have been collected at locations across the US located in key geographic areas and provide considerable insight about how AER values vary across the US. Within the indoor air quality community, many research analyses have been published (Table 3) to evaluate these datasets recognizing that AERs are a key determinant in understanding inhalation exposures.

Characteristic examples of US residential AER distributions are presented in Table 3 and Figure 2. In Figure 2, Isaacs' study is presented with curves for Detroit as the data for this case account for the greatest variability in AER values. Values for the other cities, indicating similar trends, are included in Table 3. The data for Murray and Burmaster²¹ and Koontz and Rector²² are shown for region 2 and Midwest cities, respectively, which include Detroit data. Koontz and Rector²² data was not reported for different seasons. Murray and Burmaster²¹ data for region 2 summer was not available.

Measured AER varies by an order of magnitude among 90% (5th to 95th percentile) of US homes due to a number of factors, including housing characteristics and meteorological conditions. AER distribution depends mainly on house age, the central air condition (AC) status and weather (e.g. season, ambient temperature and humidity, wind speed and direction, and climate zone). Older^{19, 23} and low income²⁰ homes, tend to have higher AERs. Conversely, homes that are newer^{19, 23} and conventional²⁰ tend to have lower AERs. AERs in homes with central AC is much lower compared to homes without central AC¹⁹. The lower AER curves were obtained in the cold weather (Figure 2). Homes without central AC in warm weather tend to have the highest AERs¹⁹. Regression analyses²³ on updated LBNL database with home built more recently predicts for whole US a slightly (15–30%) higher NL values compared to previous study²⁰, as well as some between-state differences that can be explained by the climate zones and the year built. USEPA's median residential AER of 0.45 is based on Koontz and Rector²². However, this median value is not representative of more recent datasets, as shown in Figure 2 and Table 3.

Factors Controlling Between-House AER Variations—The AER variations across residences in the same geographical region are due to differences in occupant behavior (e.g., opening windows, operating mechanical ventilation, indoor temperature from thermostat setting during heating and cooling seasons), and building characteristics (e.g., leakage of building envelope, type of mechanical ventilation)^{18,24–25}. For residences in different geographical regions, the AER variations can also include differences in wind speed (near coast versus inland) and outdoor temperature¹⁸.

Continuous measuring of AER in single home during a VI study indicated slow seasonal oscillation accompanied by daily brief transients (e.g., positive and negative spikes)². The seasonal AER temporal variations are primary due to variations of the indoor-outdoor temperature differences while the spikes correspond primarily to the wind speed variations, and secondarily to indoor-outdoor temperature difference variations. Generally, temporal AER variability of individual homes tends to decrease with decreasing median AER (e.g., tighter building envelop)²⁵.

RELEVANCE FOR VI STUDIES

IA concentrations calculated using Equation 8 with recent AER values (Table 3) and 3D VI model simulations (\dot{m}_i) demonstrate the importance of AER uncertainty on VI exposure risks. Equation 8 is a slight revision to Equation 1, reflecting the new understanding that Q_{ck} in Eq. 1 is included in the formal definition of AER as defined by the *ASHRAE Handbook* -

*Fundamentals*¹⁷. Equation 8 also explicitly accounts for chemical entry via exchanged air, if chemicals are present.

$$C_{indoor} = \frac{\dot{m}_i}{AER \cdot V_b} = \frac{\dot{m}_i}{Q_b} \quad (8)$$

Where, the mass flowrate of “i” into building (\dot{m}_i) (M/t) is given by:

$$\dot{m}_i = J_T A_{ck} + C_{i,ex} AER \cdot V_b + \dot{m}_{i,other} \quad (9)$$

Where,

Q_b – total flowrate through the building, which as discussed previously includes a combination of infiltration and ventilation (both mechanical and natural) (L^3/t).

$C_{i,ex}$ – chemical “i” concentration in exchanged air (M/L^3)

$\dot{m}_{i,other}$ – Mass flowrate of “i” into the building from sources other than VI and exchanged air. Similar formulation for \dot{m}_i was provided by others¹⁴.

For the purpose of the current study we assume that the only source of chemical “i” is the soil gas mass entry rate ($J_T A_{ck}$) and the chemical concentration in exchanged air or from other sources is equal to zero ($C_{i,ex} AER \cdot V_b + \dot{m}_{i,other} = 0$). As discussed above, AER (in the denominator of equation 8) is notably influenced by the stack and wind effects. The mass entry rate of contaminant into buildings (the numerator in equation 8) is theoretically influenced by these two factors, as well. However, there are currently no VI models that adequately account for stack and wind effects in both the numerator and the denominator in Equation 8. In fact, this is an active area of research for the authors and others. Therefore, to gain the mass entry rate, the research herein used a VI modeling approach that has been widely published²⁸ and has been compared to field data⁴.

Single Building and Single Geology Evaluation

Figure 3 illustrates the effect of AER on a hypothetical single VI site where the geology is modeled as sandy soil ($K = 10^{-11} \text{ m}^2$). IA concentrations were calculated using equation 8 and the AER values in this equation were taken from Isaacs *et al.*¹⁹ for Detroit, MI (Table 3 and Figure 2). The soil gas mass entry rate was calculated using a 3-D VI model for the base scenario described by Pennell *et al.* that includes a single building (10 m × 10 m) with a basement (2 m deep) located in the center of an open field and depressurized (-5Pa)²⁸. Therefore, the mass entry rate in equation 8 was a constant across all scenarios in Figure 3. The results show greater C_{indoor}/C_{source} variability for warm weather compared to cold weather. The age of the house affected C_{indoor}/C_{source} by an order of magnitude (1.9×10^{-3} to 2.4×10^{-4}), indicating the older homes had lower C_{indoor}/C_{source} due to higher AERs. AC operational status resulted in more than one order of magnitude variability of C_{indoor}/C_{source}

(4.4×10^{-3} to 1.2×10^{-4}). Previously field study data has reported similar observations for IA concentrations and AC status³.

AER Distribution and VI Field Data Comparison

Figure 4 illustrates the combined effect of an AER distribution that considers important building features within four geographic areas; and compares AER values to the USEPA VI Database. The need for a geographically diverse AER distribution that is a product of different home types, climate regions and weather conditions in US was a consequent of our goal to compare theoretical evaluations to USEPA VI database⁴⁴. The soil gas mass entry rate was calculated using a 3-D VI model described above and considered sand, sandy loam, and clay loam geologies with a building depressurized (-5Pa). In addition, it considered a diffusion only VI scenario depressurization (0Pa)

The AER distribution, presented in Figure 5, combines the sixteen final categories distributions, given in Isaacs *et al.*¹⁹ and summarized in Table 3, using the weighted average formulation:

$$A_j = \frac{\sum_{i=1}^{16} A_{i,j} N_i}{\sum_{i=1}^{16} N_i} \quad (10)$$

Where,

A_j - Combined AER value corresponding to percentile j (5, 25, 50, 75, 95),

$A_{i,j}$ - AER value for case i (1–16) and percentile j,

N_i – Number of observation in case i.

Currently, USEPA's VI Database represents the largest collection of VI data for chlorinated VOCs in the US; containing 2929 paired measurements from 42 vapor intrusion sites across the country though the majority of sites are from the North-east and Western portions of the country⁴⁴. Groundwater attenuation factor ($C_{\text{indoor}}/C_{\text{source}}$) distribution (5th to 95th percentile) with a filter of groundwater VOCs 1000 times greater than background VOCs (Table 7, USEPA⁴⁴), presented in Figure 6, show that 90% of groundwater attenuation factors vary over three orders of magnitude.

The results shown in Figure 4 suggests that the combined effect of AER and geology provide a possible explanation for 90% of the variability in the EPA database; and strongly supports the need to consider the implications of AERs when making decisions at VI sites. The simplest approach is to select AER measured value based on various factors (e.g., building characteristics, season, and geographical region) most similar to the investigated case. The main limitation is the uncertainty of using AER measurements from other buildings and from sampling periods with different weather conditions, natural ventilation, and mechanical ventilation.

AER Measurement Methods

Building science and air quality science provide well established methods for estimating single home AER^{17–26, 45–50} that can be implemented as part of VI site investigations. One of the more robust techniques for measuring the actual AER of a building is using a tracer gas dilution method^{16,17,45}, but measuring the actual AER is often limited due to costs of collecting site-specific field data, participant burden, and building access restrictions^{18, 24}. Further, these methods are sensitive to current weather conditions¹⁸. Alternatively, AER can be estimated using “equivalent leakage area” methods, which compared to AER measuring methods are typically less expensive^{18, 24}, easier and are similar to methods being implemented to measure VI fluxes into buildings^{11–13}. However, leakage area methods only capture infiltration rates; therefore in order to estimate the total AER, numerical models must be incorporated. The section below describes leakage area measurement methods for a single-zone approach based on the assumption of a single, well mixed enclosure. Airflow between internal zones and between the exterior and individual internal zones has led to the development of multi-zone measurement techniques. A recent study suggests that multi-zone air leakage considerations may play important roles in indoor air quality models⁵¹; however, these multi-zone measurement techniques are complex and beyond the scope of this review.

Air Leakage Area Measuring Method

The air leakage of a building characterizes the relationship between pressure difference (P) across the building envelope and the airflow through it; and is an indication of building tightness. Leakier buildings will require higher airflow rates to pressurize the building to a certain level, whereas tighter buildings will require lower flow rates.

Air leakage of a building is measured with pressurizing test known as “Blower Door” test^{47,52–53}. A large fan or blower is mounted in a door or window and induces a large, roughly uniform P across the building shell. This test is performed with natural ventilation openings closed and mechanical ventilation turned off. Airflow (through a calibrated orifice) is adjusted to generate various indoor–outdoor pressure difference (P). The experimental results provide an estimate of the area of an opening which would be equivalent in size to lumping all the combined openings throughout the structure into one opening. This opening area is used in AER models described below.

Most commonly, airflow is measured at $P=50$ Pa, which is insensitive to the influence of wind variation during the test, and therefore provides reproducible data sets. The resulting AER at 50 Pa (AER50) is calculated by dividing the resulting flow rate by the building volume. AER50 is a useful metric for comparing houses of different sizes and is used as an input for the SF leakage model.

The Lawrence Berkeley Laboratory (LBL) infiltration model⁴⁸ and its extended version that include natural ventilation (LBLX)²⁴ uses the Effective Leakage Area (ELA) of a building, wind speed, and inside-outside temperature differences to estimate the AER.. The LBLX model will be described in a later section. The ELA of a building is defined as the area of a calibrated orifice that would have the same air flowrate as the house at a reference standard

pressure of 4 Pa. ELA is an estimate of the combined size of all the leaking areas in the building.

ELA is measured using the multipoint test where blower door flowrates, at a series of P_s ranging from about 10–70 Pa, are measured to determine the relationship between P and leakage rate for the test home (Q_f). Equation 6 is used to find κ and n based on the best fit of the data. Since ELA depends on the indoor–outdoor P , it is necessary to extrapolate experimental results to determine the ELA at the reference pressure (P_r).

The relationship between the airflow rate through the fan orifice and the P can be expressed as:

$$Q_f = ELA \sqrt{2\Delta P / \rho} \quad (11)$$

Combining and rearranging Eq. 6 and 11 allow determination of ELA at standard reference pressure:

$$ELA = (\sqrt{\rho/2}) \kappa P_r^{(n-0.5)} \quad (12)$$

There is uncertainty in ELA estimation which is due to 1) measurement errors and 2) model specification. Wind can be a source of measurement errors when pressure and flowrate are measured during pressurization test. The model specification error can be created by extrapolation to measure the flowrate at 4 Pa^{54–55}. Walker et al. (2013) compared single point and multipoint testing approaches and showed that the multipoint testing described above is recommended for the conditions when there is a wind speed less than 6 m/s during the test. For wind speeds greater than 6 m/s, they suggest a single point testing at $P=50$ Pa with a fixed pressure exponent ($n=0.65$) which is less sensitive to wind pressure fluctuations and cause reduction in experimental errors⁵⁶.

AER Estimation Models

AER estimation models can be distinguished broadly into two categories; empirical models (e.g., data-driven approaches) and physically based models (e.g., based on fundamental physical theory). The physically-based models have been classified into: 1) single zone models and 2) multi-zone models. Various AER models have been described in the literature^{17–18}. Selected models are described briefly below.

Empirical model

The SF model is an empirical model that relates the AER at 50 Pa (AER50) to AER at typical natural conditions (4 Pa) using a scaling factor (F) as:

$$AER_{SF} [h^{-1}] = \frac{AER50}{F} \quad (13)$$

Chan *et al.*²⁰ found that $F = 16$ gives the best fit for the national data. A commonly used metric for building leakage is the Normalized Leakage, NL, defined as:

$$NL = 1000 \cdot \frac{ELA}{A_{\text{floor}}} \frac{H}{2.5}^{0.3} \quad (14)$$

Where,

A_{floor} – Floor area (L^2)

H - The height of the building (L)

NL is ELA normalized with the building floor area and a correction factor for the building height.

It describes the relative leakage for a wide range of building sizes²⁰. To describe AER50 in terms of NL Eqs. 6, 11, and 14 are combined to yield:

$$AER50 [h^{-1}] = 48 \left(\frac{2.5m}{H} \right)^{0.3} \frac{NL}{H} \quad (15)$$

NL can also be estimated from leakage area model such as²⁰:

$$NL = \exp(\beta_0 + \beta_1 y_{\text{built}} + \beta_2 A_{\text{floor}}) \quad (16)$$

Where,

Y_{built} – year of construction

β_0 , β_1 and β_2 - regression parameters, which were estimated for three housing types: low income, conventional, and energy efficient²⁰.

A comparison of AER distribution curves measured with the PFT method (Isaacs) and AER_{SF} based on air leakage method (Chan), given in Figure 7, show a good agreement between the two distributions; Isaacs's newer homes curve is very close to Chan's conventional curve, and Isaacs's older homes curve is very close to Chan's low income curve. Figure 7 supports the use of the SF model with air leakage measurement. Additionally, the SF model was evaluated with data from 642 daily (e.g., 24 h average) AER measurements across 31 detached homes in central North Carolina collected on seven consecutive days during each of four consecutive seasons and showed a median absolute difference of 50% (0.25 1/h), a slightly higher compared to physical based more sophisticated models (e.g., a median absolute difference of 43% (0.17 1/h) and 40% (0.17 1/h) for the LBL and LBLX models, respectively)²⁴. The main limitation of this simple model is the absent of sensitivity for meteorological conditions (e.g., stack and wind effects) and thus for hourly variations as well.

Simplified single-zone models

LBL and LBLX model—The LBL model is widely used as a tool for predicting residential infiltration rates.^{17,48} Stack and wind effects, the driving forces for infiltration, are calculated separately, and then combined using superposition.⁵⁰ The LBL model has been compared to AERs measured by tracer gas technique, which were measured during different time periods and different seasons. These comparisons showed that the LBL model predictions resulted in mean absolute errors of 25–46%^{24, 25, 57,58}.

LBLX model is an extended version of LBL model that includes natural ventilation airflow through large intentional openings (e.g., windows, doors)²⁴. The LBLX model predicts the AER due to infiltration and natural ventilation. The median absolute difference between LBLX model prediction, using Eq. 16 for leakage area, and data from 642 daily AER measurements across 31 detached homes in central North Carolina, with corresponding window opening and meteorological data was 40% (0.17 1/h)²⁴, and 29% (0.19 1/h) for data from a subset of 24 study homes on five consecutive days during two seasons in Detroit MI²⁵.

Multizone air flow models

Several multizone computational models have been developed to calculate air flows and contaminant distribution in multizone buildings⁵⁹. In multizone models the building is divided into several zones (e.g. rooms) and each zone is assumed as a well-mixed zone to have uniform temperature, pressure and contaminant concentration. Zones are connected to each other by flow paths (e.g. cracks, openings, ducts). Two examples of well-known multizone air flow models are CONTAM and COMIS. CONTAM⁶⁰ was developed by the “Building and Fire Research Laboratory of the National Institute of Standards and Technology” (NIST). COMIS⁶¹ was developed by an international group of experts (the Energy Performance of Buildings Group) at the Lawrence Berkeley National Laboratory. In both of these models, wind effect, stack effect and mechanical ventilation are taken into account in building air flow estimation.

COMIS⁶¹, like CONTAM⁶⁰, uses a similar procedure in solving air flow rates through openings of a building. Both models use a conservation of mass in all zones to calculate the zonal pressures and air flow rates through flow paths. CONTAM and COMIS use dimensionless pressure coefficients and Bernoulli’s equation to gain the pressure distribution on building surfaces induced by wind speed and direction. These two models are widely used in indoor air quality studies and could be used in VI studies to estimate the total air exchange rate of the building and also indoor air concentration of contaminant considering air flows through the building induced by infiltration, natural and mechanical ventilation⁵⁹.

CONCLUSIONS AND IMPLICATIONS

AERs commonly referenced in VI literature (Table 1) are not representative of the wider range of values present in IA quality literature (Table 3 and Figure 5). IA concentration data collected during VI investigations should be interpreted by considering how AERs may influence the measured IA concentration data. As show in Equation 8, IA concentrations

may be diluted by high AERs; if building operation is modified by a building occupant behavior and the AER is decreased, the IA concentration may respond by increasing.

An inaccurate assumption that AERs fall within USEPA's conservative screening range (0.18–1.26 1/h) could result in a false understanding that residential buildings across the US have AERs within this narrow range. However, as shown on Figure 5, recent literature reports a broader range (up to 6.1 1/hr). While the majority of AERs do not deviate substantially from USEPA's conservative screening range, careful consideration is warranted by the VI scientific community when evaluating and interpreting measured IA concentrations as part of VI site assessments.

VI communities continue to be impacted by decisions at VI sites, even after VI site specific risk assessments are completed. Therefore, as part of the USEPA multiple lines of evidence approach, practitioners and regulators should consider how building characteristics may influence AERs and VI exposures risks. The *ASHRAE Handbook - Fundamentals*¹⁷ highlights several building features that are known to influence AERs. For instance, older windows and doors, building penetrations, fireplaces, *etc.* are features that may increase infiltration. Bailly *et al.*³⁶ summarizes the results of 65,000 air tightness tests conducted in Europe and reports several leak-prone characteristics for various building-types. Practitioners should consider these qualitative factors when making decisions and communicating risks at VI sites. In the absence of well-known ventilation rates, specific trends about the building's AER cannot be easily extracted based on leakage information alone. However, leak-prone building features may play a role in potentially decreasing IA concentrations and these features can be identified and evaluated as part of VI investigations.

Mechanical and natural ventilation are also an important part of AERs. The exact contribution of ventilation to the total AER is not easily estimated. There may be a need to consider the role of occupant behavior on natural (*e.g.* open windows and doors) and mechanical ventilation systems, such as bathroom and kitchen exhaust fans. The VI community has not routinely considered the variability of ventilation systems during VI investigations. Most IA sampling is conducted during heating seasons, when windows and doors are closed to limit natural ventilation and when AERs are thought to be low (most conservative); however even during "cold seasons" some regions of the US have been shown to have AERs > 4 1/hr (see New Jersey data, Table 3).

Further, AERs of buildings can vary considerably based on age and construction. Isaacs *et al.*¹⁹ showed that AERs for newer and older homes during heating seasons (*e.g.* "cold" data) varied as much as a factor of 4 for the 95 percentile (see New Jersey data, Table 3), with the older homes having the higher AERs (less conservative values). Importantly, Chan *et al.*²⁰ (Table 3) showed "low income" homes had higher AERs (less conservative values). These are important implications to consider when evaluating VI exposure risks at VI sites.

Risk management and communication at VI sites should continue to highlight the dynamic nature of VI exposure risks. Decisions that do not consider the possibility of higher AERs to decrease IA concentrations, may not be conservative in terms of future VI exposure risks. For example, energy-efficiency initiatives that target older homes and low-income

areas e.g.⁶² may reduce AERs at buildings after VI assessments have deemed IA concentrations are below risk levels. With many energy efficiency programs being implemented in neighborhoods, these types of temporal changes in AERs (and ultimately changes in VI exposure risks) should be considered. If a homeowner makes future modifications, perhaps as part of a weatherization program (or any other optional home improvement), the IA concentration may change. VI practitioners should engage in risk communication plans that communicate these types of related building issues to homeowners and regulators should consider follow up sampling requirements.

Field measurements could provide information to contextualize IA concentration data. VI practitioners may consider measuring building air leakage area to calculate infiltration in homes where vapor intrusion may be occurring. This information combined with knowledge about, or measurements of, building ventilation may inform vapor intrusion decisions. However, occupant behaviors that could influence building ventilation rates and influence IA concentrations should also be considered.

As discussed above, building features and other factors that influence AER should be taken into account when evaluating IA concentrations as part of the multiple lines of evidence approach at VI sites. Decisions about whether to qualitatively, and/or quantitatively consider AERs can be made on a case-by-case basis within the framework of the specific context of the exposure scenario.

Lastly, AERs are influenced by some of the factors that influence soil gas entry into buildings (wind and indoor-outdoor temperature differential (stack effect)). More research is needed to understand how above-ground and subsurface processes are coupled. This is an active area of research. While research results continue to emerge, VI practitioners can use multiple lines of evidence to make the best decisions possible given the information and evidence currently available.

Acknowledgments

The authors appreciate the thoughtful input and constructive comments of the reviewers. The project described was supported by Grant Number P42ES007380 (University of Kentucky Superfund Research Program) from the National Institute of Environmental Health Sciences and by Grant Number 1452800 from the National Science Foundation. The content is solely the responsibility of the authors and does not necessarily represent the official views of the National Institute of Environmental Health Sciences, the National Institutes of Health or the National Science Foundation.

References

1. U.S. Environmental Protection Agency. OSWER technical guide for assessing and mitigating the vapor intrusion pathway from subsurface vapor sources to indoor air. Environmental Protection Agency; Washington, DC: 2015.
2. Holton C, Luo H, Dahlen P, Gorder K, Dettenmaier E, Johnson PC. Temporal variability of indoor air concentrations under natural conditions in a house overlying a dilute chlorinated solvent groundwater plume. *Environ Sci Technol*. 2013; 47:13347–13354. DOI: 10.1021/es4024767 [PubMed: 24180600]
3. Johnston JE, Gibson JM. Spatiotemporal variability of tetrachloroethylene in residential indoor air due to vapor intrusion: a longitudinal, community-based study. *J Exposure Sci Environ Epidemiol*. 2014; 24:564–571. DOI: 10.1038/jes.2013.13

4. Pennell KG, Scammell MK, McClean MD, Suuberg EM, Moradi A, Roghani M, Ames J, Friguglietti L, Indeglia PA, Shen R, Yao Y, Heiger-Bernays WJ. Field data and numerical modeling: a multiple lines of evidence approach for assessing vapor intrusion exposure risks. *Sci Total Environ.* 2016; 556:291–301. DOI: 10.1016/j.scitotenv.2016.02.185 [PubMed: 26977535]
5. Yao Y, Suuberg EM. A review of vapor intrusion models. *Environ Sci Technol.* 2013; 47:2457–2470. DOI: 10.1021/es302714g [PubMed: 23360069]
6. Moradi A, Tootkaboni M, Pennell KG. A variance decomposition approach to uncertainty quantification and sensitivity analysis of the Johnson and Ettinger model. *J Air Waste Manag Assoc.* 2015; 65:154–164. DOI: 10.1080/10962247.2014.980469 [PubMed: 25947051]
7. Mosley, RB. Use of radon to establish a building-specific sub-slab attenuation factor for comparison with similar quantities measured for other vapor intrusion contaminants. Presented at the National Environmental Monitoring Conference; Cambridge, MA. August 2007; p. 19–25.
8. U.S. Environmental Protection Agency. Assessment of mitigation systems on vapor intrusion: Temporal trends, attenuation factors, and contaminant migration routes under mitigated and non-mitigated conditions. Environmental Protection Agency; Washington, DC: 2015. EPA/600/R-13/241
9. Shen R, Subberg EM. Impacts of changes of indoor air pressure and air exchange rate in vapor intrusion scenarios. *Building and Environ.* 2016; 96:178–187. DOI: 10.1016/j.buildenv.2015.11.015
10. Song S, Schnorr BA, Ramacciotti FC. Quantifying the influence of stack and wind effects on vapor intrusion. *Hum Ecol Risk Assess.* 2014; 20(5):1345–1358. DOI: 10.1080/10807039.2013.858530
11. McHugh TE, Beckley L, Bailey D, Gorder K, Dettenmaier E, Rivera-Duarte I, Brock S, MacGregor IC. Evaluation of vapor intrusion using controlled building pressure. *Environ Sci Technol.* 2012; 46:4792–4799. DOI: 10.1021/es204483g [PubMed: 22486634]
12. Guo Y, Holton C, Luo H, Dahlen P, Gorder K, Dettenmaier E, Johnson PC. Identification of alternative vapor intrusion pathways using controlled pressure testing, soil gas monitoring, and screening model calculations. *Environ Sci Technol.* 2015; 49:13472–13482. DOI: 10.1021/acs.est.5b03564 [PubMed: 26458025]
13. Dawson, H. [accessed September 2016] Mass flux characterization for vapor intrusion assessment, ER-201503. DoD's environmental research programs. 2016. <https://www.serdp-estcp.org/Program-Areas/Environmental-Restoration/Contaminated-Groundwater/Emerging-Issues/ER-201503>
14. Luo, H. PhD thesis. Arizona State University; Tempe, AZ: 2009. Field and modeling studies of soil gas migration into buildings at petroleum hydrocarbon impacted sites.
15. Reichman R, Roghani M, Willett EJ, Shirazi E, Pennell KG. Air exchange rates and alternative vapor entry pathways to inform vapor intrusion exposure risk assessments. *Reviews on Environmental Health.* [Accepted, September 2016]
16. U.S. Environmental Protection Agency. Exposure Factors Handbook – 2011 Edition. Office of Research and Development; Washington, D.C: 2011. EPA/600/R-090/052F www.epa.gov/ncea/efh/pdfs/efh-complete.pdf [accessed September 2016]
17. American Society of Heating, Refrigerating and Air conditioning Engineers. Handbook of Fundamentals. ASHRAE Inc; Atlanta, GA: 2013.
18. Breen MS, Schultz BD, Sohn MD, Long T, Langstaff J, Williams R, Isaacs K, Meng QY, Stallings C, Smith L. A review of air exchange rate models for air pollution exposure assessments. *J Exposure Sci Environ Epidemiol.* 2014; 24:555–563. DOI: 10.1038/jes.2013.30
19. Isaacs K, Burke J, Smith L, Williams R. Identifying housing and meteorological conditions influencing residential air exchange rates in the DEARS and RIOPA studies: development of distributions for human exposure modeling. *J Exposure Sci Environ Epidemiol.* 2013; 23:248–258. DOI: 10.1038/jes.2012.131
20. Chan W, Nazaroff W, Price P, Sohn M, Gadgil A. Analyzing a database of residential air leakage in the United States. *Atmos Environ.* 2005; 39:3445–3455. DOI: 10.1016/j.atmosenv.2005.01.062
21. Murray DM, Burmaster DE. Residential air exchange rates in the United States: empirical and estimated parametric distributions by season and climatic region. *Risk Anal.* 1995; 15:459–465.
22. Koontz, MD., Rector, HE. Estimation of distributions for residential air exchange rates. U.S. Environmental Protection Agency; 1995.

23. Chan WR, Joh J, Sherman MH. Analysis of air leakage measurements of US houses. *Energy and Buildings*. 2013; 66:616–625.
24. Breen MS, Breen M, Williams RW, Schultz BD. Predicting residential air exchange rates from questionnaires and meteorology: Model evaluation in central North Carolina. *Environ Sci Technol*. 2010; 44:9349–9356. [PubMed: 21069949]
25. Breen MS, Burke JM, Batterman SA, Vette AF, Godwin C, Croghan CW, Schultz BD, Long TC. Modeling spatial and temporal variability of residential air Exchange rates for the near-road exposures and effects of urban air pollutants study (NEXUS). *Int J Environ Res Public Health*. 2014; 11:11481–11504. DOI: 10.3390/ijerph111111481 [PubMed: 25386953]
26. Baxter LK, Stallings C, Smith L, Burke J. Probabilistic estimation of residential air exchange rates for population-based human exposure modeling. *J Expos Sci Environ Epidemiol*. 2016; doi: 10.1038/jes.2016.49
27. Pennell KG, Scammell MK, McClean MD, Ames J, Weldon B, Friguglietti L, Suuberg EM, Shen R, Indeglia PA, Heiger-Bernays WJ. Sewer gas: an indoor air source of PCE to consider during vapor intrusion investigations. *Ground Water Monit Rem*. 2013; 33(3):119–126.
28. Pennell KG, Bozkurt O, Suuberg EM. Development and application of a three-dimensional finite element vapor intrusion model. *J Air Waste Manage Assoc*. 2009; 59(4):447–460. DOI: 10.3155/1047-3289.59.4.447
29. U.S. Environmental Protection Agency. Conceptual Model Scenarios for the Vapor Intrusion Pathway. Environmental Protection Agency; Washington, DC: 2012. EPA-530-R-10-003 www.epa.gov/oswer/vaporintrusion/documents/vi-cms-v11final-2-24-2012.pdf [accessed September 2016]
30. Johnson PC. Identification of application-specific critical inputs for the 1991 Johnson and Ettinger vapor intrusion algorithm. *Ground Water Monitoring and Remediation*. 2005; 25(1):63–78. DOI: 10.1111/j.1745-6592.2005.0002.x
31. Yao Y, Shen R, Pennell KG, Suuberg EM. A numerical investigation of oxygen concentrations dependence on biodegradation rate laws in vapor intrusion. *Environ Sci: Processes Impacts*. 2013; 15(12):2345–2354. Note: Spelled incorrectly as “Pennel” by journal.
32. Shen R, Yao Y, Pennell KG, Suuberg EM. Modeling quantification of the influence of soil moisture on subslab vapor concentration. *Environ Sci: Processes Impacts*. 2013; 15(7):1444–1451.
33. U.S. Environmental Protection Agency. User’s guide for evaluating subsurface vapor intrusion into buildings. Environmental Protection Agency; Washington, DC: 2004. EPA-68-W-02-33 www.dtsc.ca.gov/AssessingRisk/upload/VI_USEPA_Users-guide.pdf [accessed September 2016]
34. Picone S, Valstar J, Van gaans P, Grotenhuis T, Rijnaarts H. Sensitivity analysis on parameters and processes affecting vapor intrusion risk. *Environ Toxicol Chem*. 2012; 31(5):1042–1052. DOI: 10.1002/etc.1798 [PubMed: 22392684]
35. Patterson BM, Davis GB. Quantification of vapor intrusion pathways into a slab-on-ground building under varying environmental conditions. *Environ Sci Technol*. 2009; 43:650–656. DOI: 10.1021/es801334x [PubMed: 19244997]
36. Bailly, A., Guyot, G., Leprince, V. 6 years of envelope airtightness measurements performed by French certified operators: analyses of about 65,000 tests. 36th AIVC Conference “Effective Ventilation in High Performance Buildings.”; Madrid, Spain. 2015.
37. ASHRAE Standard 62.2–2010: Ventilation and Acceptable Indoor Air Quality in Low-Rise Residential Buildings. 2010
38. Russell M, Sherman M, Rudd A. Review of Residential Ventilation Technologies. *HVAC&R Research*. 2007; 13:325–348.
39. Stratton, JC., Iain, SW., Craig, PW. Measuring Residential Ventilation System Airflows: Part 2 - Field Evaluation of Airflow Meter Devices and System Flow Verification. 2012.
40. Howard-Reed C, Wallace LA, Ott WR. The effect of Opening Windows on Air Change Rates in Two Homes. *J Air Waste Manag Assoc*. 2002; 52:147–159. [PubMed: 15143789]
41. Jeong B, Jeong J-W, Park JS. Occupant behavior regarding the manual control of windows in residential buildings. *Energy and Buildings*. 2016; 127:206–216.

42. Walker IS, Wilson DJ. Field validation of algebraic equations for stack and wind driven air infiltration calculations. HVAC&R Research. 1998; 4:119–139.
43. Hurel N, Sherman MH, Walker IS. Sub-additivity in combining infiltration with mechanical ventilation for single zone buildings. Building and Environment. 2016; 98:89–97.
44. U.S. Environmental Protection Agency. EPA’s vapor intrusion database: evaluation and characterization of attenuation factors for chlorinated volatile organic compounds and residential buildings. Environmental Protection Agency; Washington, DC: 2012. EPA-530-R-10-002 www.epa.gov/oswer/vaporintrusion/documents/OSWER_2010_Database_Report_03-16-2012_Final.pdf [accessed September 2016]
45. American Society of Testing and Materials. ASTM, Standard E741. 2006. Standard test method for determining air change in a single zone by means of a tracer gas dilution.
46. Sherman, MH., Walker, IS., Lunden, MM. Uncertainties in air exchange using continuous-injection, long-term sampling tracer gas methods, LBNL-6544. Lawrence Berkeley National Laboratory; Berkeley, CA: 2013.
47. Sherman MH. The use of blower-door data. Indoor Air. 1995; 5(3):215–224.
48. Sherman MH, Grimsrud DT. Infiltration-pressurization correlation: simplified physical modeling. ASHRAE Transactions. 1980; 86(2):778–803.
49. American Society of Heating, Refrigerating and Air conditioning Engineers. ASHRAE Standard 119. 1988. Air leakage performance for detached single-family residential buildings.
50. Sherman MH. Superposition in infiltration modeling. Indoor Air. 1992; 2(2):101–114.
51. Guyot G, Ferlay J, Gonze E, Woloszyn M, Planet P, Bello T. Multizone air leakage measurements and interactions with ventilation flows in low-energy homes. Building and Environment. 2016; 107:52–63. DOI: 10.1016/j.buildenv.2016.07.014
52. ISO 9972:2015. Thermal performance of buildings – Determination of air permeability of buildings – Fan pressurization method. Geneva: ISO; 2015.
53. American Society for Testing and Materials. ASTM E779-10 Standard test method for determining air leakage rate by fan pressurization.
54. Sherman M. A power-law formulation of laminar flow in short pipes. Journal of Fluids Engineering. 1992; 114:601–605.
55. Sherman, M., Palmiter, L. Airflow performance of building envelopes, components, and systems. ASTM International; 1995. Uncertainties in fan pressurization measurements.
56. Walker I, Sherman M, Joh J, Chan W. Applying Large Datasets to Developing a Better Understanding of Air Leakage Measurement in Homes. International Journal of Ventilation. 2013; 11:323–338.
57. Palmiter, L., Francisco, PW. Modeled and measured Infiltration Phase III: A detailed case study of three homes. Ecotope Inc; Seattle, WA: 1996. (Technical Report)
58. Wang W, Beausoleil-Morrison I, Reardon J. Evaluation of the Alberta air infiltration model using measurements and inter-model comparisons. Build Environ. 2009; 44:309–318.
59. Wang H, Zhai ZJ. Advances in building simulation and computational techniques: A review between 1987 and 2014. Energy and Buildings. 2016; 128:319–335.
60. Dols, WS., Polidoro, BJ. CONTAM User Guide and Program Documentation Version 3.2. 2015. <http://www.bfrl.nist.gov/IAQanalysis/docs/nist-tn-1887-v3202.pdf>
61. Feustel HE. COMIS—an international multizone air-flow and contaminant transport model. Energy and Buildings. 1999; 30:3–18.
62. Cluett, R., Amann, J., Ou, S. Building better energy efficiency programs for low-income households. American Council for an Energy-Efficient Economy; Washington DC: Mar. 2016 Report Number A1601

ENVIRONMENTAL IMPACT STATEMENT

This tutorial review draws connections between the well-established yet disparate fields of subsurface vapor intrusion (VI) and building air exchange rate (AER) studies. The main purpose of this review is to grow awareness within the VI scientific community about the potential importance of AERs when evaluating VI exposure risks. We show that AERs commonly referenced by the VI community are not representative of the wider range of AER values reported within the IA quality literature. A summary of recent AER values from the IA quality literature are summarized and implications for VI exposure risk assessment are discussed.

Author Manuscript

Author Manuscript

Author Manuscript

Author Manuscript

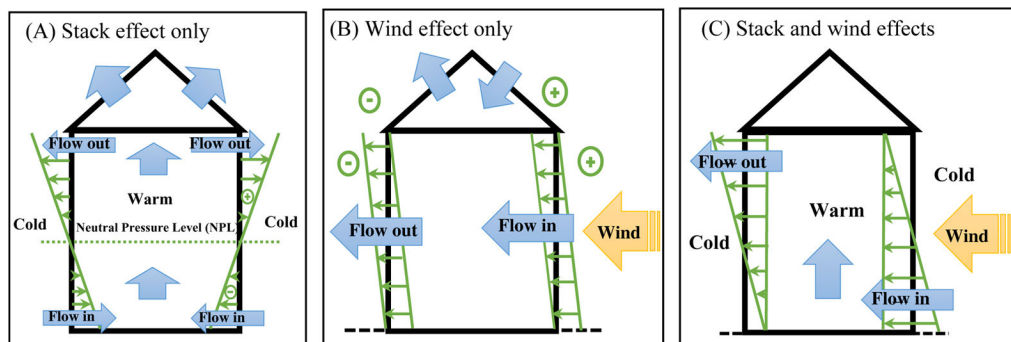


Figure 1. Distribution of inside and outside pressures (green arrows) over height of a building, and airflow directions (blue arrows) for; (A) Stack effect only for case where inside air is warmer than outside air (winter) and NPL is at the mid-height, (B) Wind effect only, and (C) Wind and stack effects combined. For simplicity of illustration pressure differences due to the wind and stack effect have the same magnitude, which is rare in reality. Adapted from *ASHRAE Handbook - Fundamentals*¹⁷

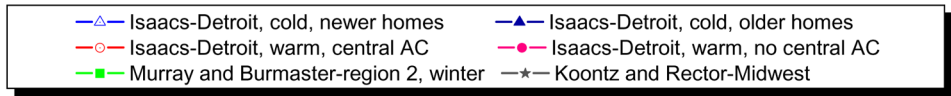
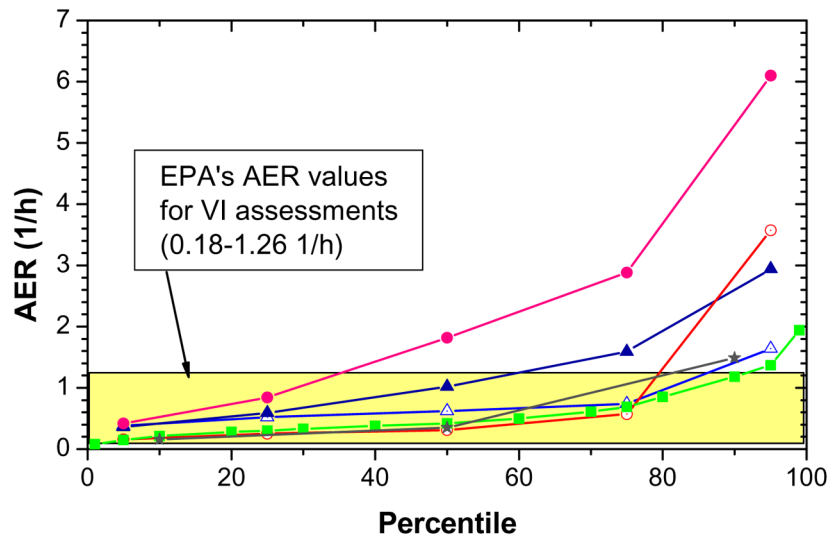


Figure 2. Characteristic examples of residential AER distribution curves.

Author Manuscript

Author Manuscript

Author Manuscript

Author Manuscript

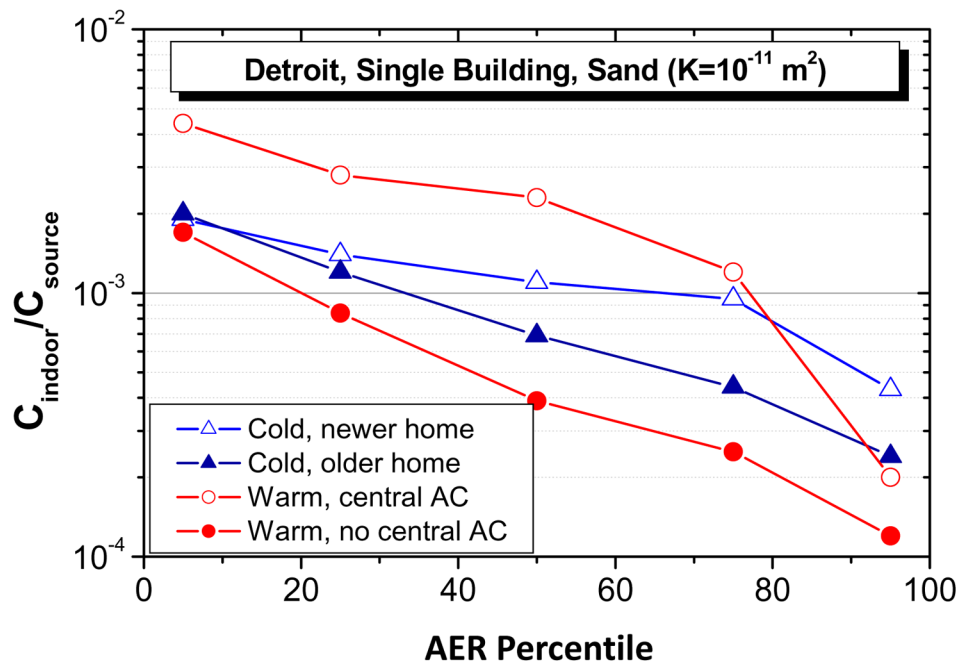


Figure 3.
AER effect on $C_{\text{indoor}}/C_{\text{source}}$ distribution curves for Detroit test case.

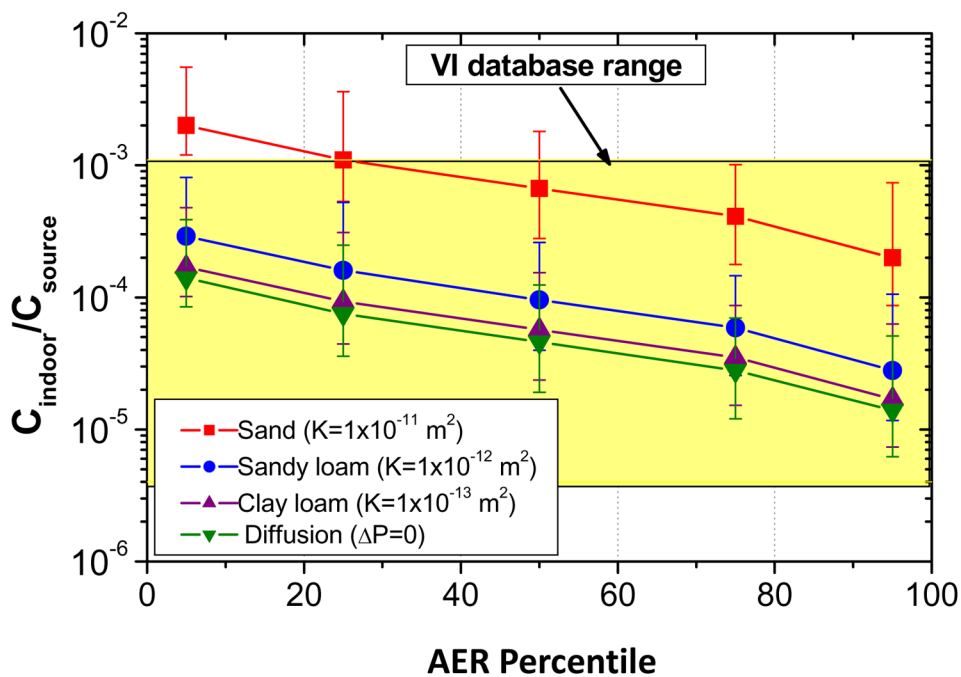


Figure 4. Combined effect of AER distribution and geology on $C_{\text{indoor}}/C_{\text{source}}$ in comparison to USEPA VI database range (shaded area). Error bar present maximum and minimum values.

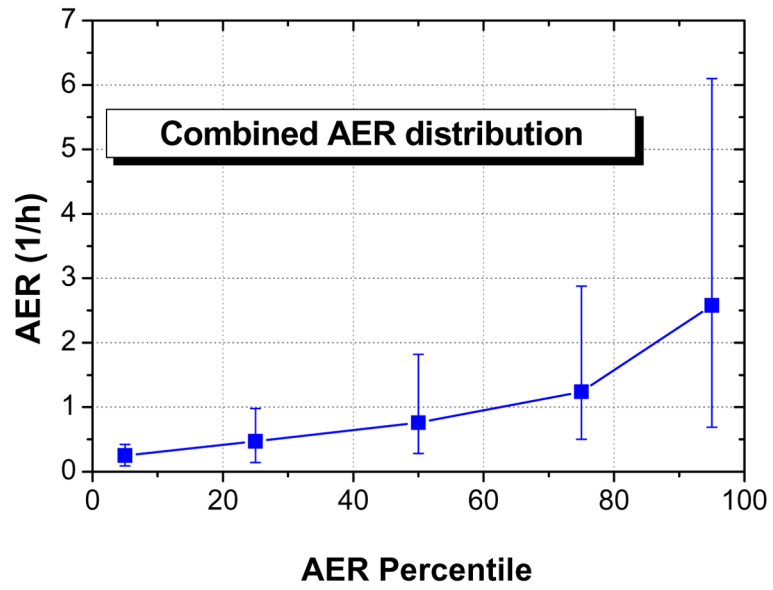


Figure 5.
AER distribution that considers important building features within four geographic areas.
The error bar show maximum and minimum values.

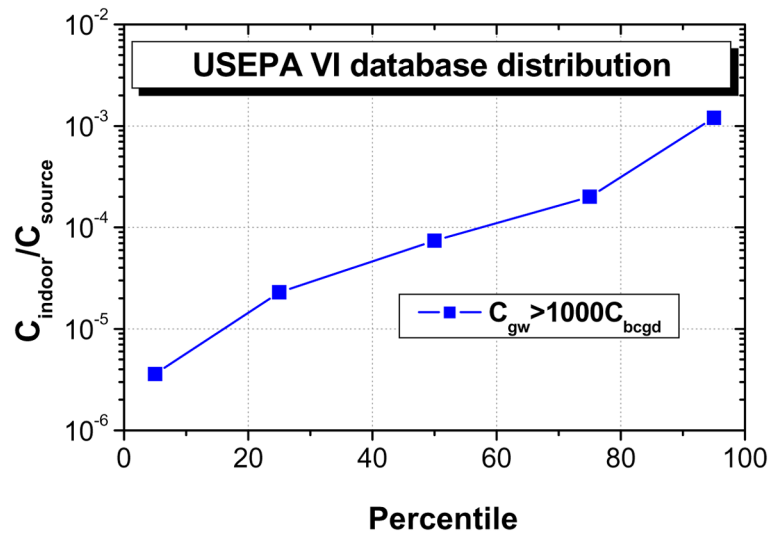


Figure 6. USEPA VI database groundwater attenuation factor ($C_{\text{indoor}}/C_{\text{source}}$) distribution (5th to 95th percentile) for a filter of groundwater VOCs 1000 times greater than background VOCs.

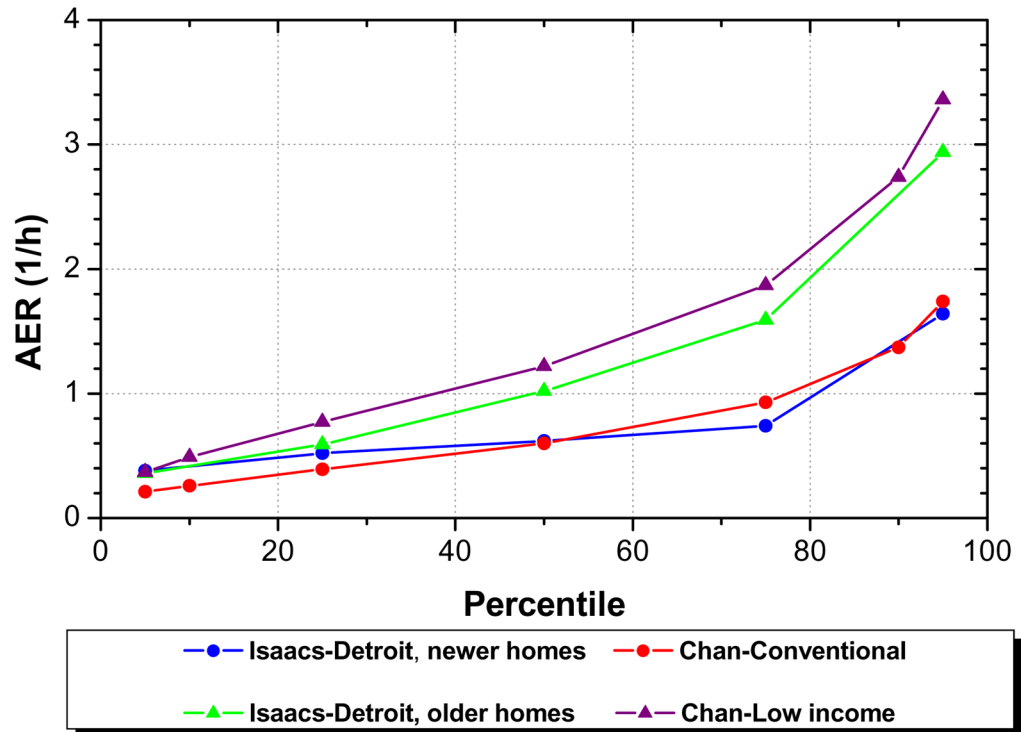


Figure 7. A comparison of AER distribution curves measured with the PFT method (Isaacs, Isaacs *et al.*¹⁹) and the air leakage method (Chan, Chan *et al.*²⁰).

Table 1

Typical Residential AER values reported in VI studies.

Study	values (h ⁻¹)	Comments
USEPA, 2015 ¹	<ul style="list-style-type: none"> • Typical range of values: 0.18 – 1.26. • Range used for developing various protocols (e.g. sampling of indoor air, soil gas, etc.): 0.25 – 1. • Values used to develop generic attenuation factors: 0.45 and 0.18. 	Values after EPA, 2011 ¹³ ; table 19–12 (after Koontz and Rector, 1995 ¹⁷).
USEPA, 2015 ⁸	<ul style="list-style-type: none"> • April/May 2011: 0.56 – 0.74 • September: 0.34 – 0.72 	Measured in a specific house (Indianapolis, IN).
EPA, 2012 ²⁹	<ul style="list-style-type: none"> • One home: 0.5. • Multiple homes: 0.25 and 1. 	Table B-1.
EPA, 2004 ³³	<ul style="list-style-type: none"> • Range of values for VI models: 0.1 – 1.5. • Default value: 0.25. 	Table 9.
Johnson, 2005 ³⁰	<ul style="list-style-type: none"> • Reasonable primary input values: 0.2–1. • For various sensitivity analysis scenarios use values: 0.6 – 1.3. 	Sensitivity analysis study.
Picone <i>et al.</i> , 2012 ³⁴	<ul style="list-style-type: none"> • Values: 0.2 and 2. 	Sensitivity analysis study.
Moradi <i>et al.</i> , 2015 ⁶	<ul style="list-style-type: none"> • Range: 0.18 – 1.26. 	Sensitivity analysis study.
Shen and Suuberg, 2016 ⁹	<ul style="list-style-type: none"> • Fall: 0 – 0.6, [0.3 + 0.3 sin(2πt/12[h])]. • Summer: 0 – 2, [1 + sin(2πt/12[h])]. 	Sensitivity analysis study.
Patterson and Davis, 2009 ³⁵	<ul style="list-style-type: none"> • Ambient building pressure, fully sealed: 0.66±0.04 • Ambient building pressure, partly sealed: 1.3±0.1 • Reduced building pressure (–12Pa): 2.0±0.1 	Measured in a specific house (Perth, Western Australia).
Holton <i>et al.</i> , 2013 ²	<ul style="list-style-type: none"> • Fall to spring months: <ul style="list-style-type: none"> – Typical daily averages: 0.6 – 1. – Instantaneous excursions: 0.4 – 1.5. • Summer: <ul style="list-style-type: none"> – Typical daily averages: 0.2 – 0.4. – Instantaneous excursions: 0.2 – 0.5. 	Measured in a specific house (Layton, UT).

Table 2

Summary of database sources for AER distribution.

Source	Description	Method
Brookhaven National Laboratory (BNL) ^{16,21}	<ul style="list-style-type: none"> Containing over 4,000 measurements for single and multifamily dwelling units. Collected during the period of 1982–1987. Various projects. 	PFT
Detroit Exposure and Aerosol Research Study (DEARS) ¹⁹	<ul style="list-style-type: none"> Homes in Wayne County Michigan. Collected during the period of 2004–2007. Two seasons: Summer (Jul–Aug), winter (Jan–Mar). A total of 128 homes: <ul style="list-style-type: none"> – Summer: 105 homes – Winter: 90 homes – Both seasons: 67 homes. 24 h monitoring period. 	PFT
Relationships in Indoor, Outdoor, and Personal Air (RIOPA) ¹⁹	<ul style="list-style-type: none"> Three US metropolitan cities located in different climate zones: Elizabeth NJ, Houston TX, and Los Angeles, CA. Collected during the period of 1999–2001. Four seasons 300 houses (about 100 homes in each city). Two seasons at each house. 48 h monitoring period. 	PFT
Lawrence Berkley National Laboratory (LBNL) ²⁰	<ul style="list-style-type: none"> Containing 73,000 measurement. Collected in 2001 and earlier. Contributors to the database: <ul style="list-style-type: none"> – Ohio Weatherization Program that include houses occupied by low income households (77%) – Energy-efficiency program in Alaska (11%) – Wisconsin Energy Conservation Corporation (3%). – Thirty-one other organizations from 30 states (9%). 	Air leakage ^a

^aNL values were converted to AER using Eq. 13

PFT - perfluorocarbon tracer method

Table 3

Typical Residential AER distribution studies.

Study	AER distribution				Database	Comments
	Category	Value (l/h)				
		10 th	50 th	90 th		
Koontz and Rector, (1995) ²²	All regions	0.18	0.45	1.26	BNL	• Analyzed 2971 measurements.
	West region	0.20	0.43	1.25		• Assigned weights to compensate for the geographic imbalance.
	Midwest region	0.16	0.35	1.49		
	Northeast region	0.23	0.49	1.33		
	South region	0.16	0.49	1.21		
	<u>Colest region (1)</u>				BNL	• Analyzed 2844 measurements.
	Winter	0.11	0.27	0.71		• Did not assign weights.
	Spring	0.18	0.36	0.80		• The climate regions were defined according to the number of annual heating degree days.
	Summer	0.27	0.57	2.01		• Winter: Dec – Feb, Spring: Mar– May, Summer: June – Aug, Fall: Sept – Nov.
	Fall	0.10	0.22	0.42		
Chan <i>et al.</i> 2005 (Chan) ²⁰	<u>Warmest region (4)</u>					
	Winter	0.24	0.48	1.13		
	Spring	0.28	0.63	1.42		
	Summer	0.33	1.10	3.28		
	Fall	0.22	0.42	0.74		
	Whole US	0.27	0.65	1.62	WAPs	• NL values were converted to AER using Eq. 13
	Low income	0.49	1.22	2.74		
	Conventional	0.26	0.60	1.37		
		5 th	50 th	95 th		
	Isaacs <i>et al.</i> 2013 (Isaacs) ¹⁹	<u>Detroit, MI</u>				DEARS
Cold, newer homes		0.38	0.62	1.64		
Cold, older homes		0.36	1.02	2.94		
Warm, central AC		0.16	0.31	3.57		
Warm, no central AC		0.42	1.82	6.10		

Author Manuscript

Author Manuscript

Author Manuscript

Author Manuscript

Study	AER distribution			Database	Comments
	Category	Value (1/h)			
		10 th	50 th	90 th	
	<u>Elizabeth, NJ</u>				RIOPA
	Cold, newer homes	0.39	0.56	1.03	
	Cold, older homes	0.32	0.76	4.14	
	Warm, central AC	0.11	0.72	1.04	
	Warm, no central AC	0.30	1.04	3.40	
	<u>Houston, TX</u>				RIOPA
	Cold, newer homes	0.09	0.28	0.69	
	Cold, older homes	0.18	0.66	2.29	
	Warm, central AC	0.13	0.38	1.10	
	Warm, no central AC	0.23	0.56	2.74	
	<u>Los Angeles, CA</u>				RIOPA
	Cold, newer homes	0.17	0.42	1.32	
	Cold, older homes	0.32	0.80	2.24	
	Warm, central AC	0.26	0.71	2.70	
	Warm, no central AC	0.21	1.45	4.35	